

Apo2L/TRAIL Inhibits Tumor Growth and Bone Destruction in a Murine Model of Multiple Myeloma

Agatha Labrinidis,¹ Peter Diamond,² Sally Martin,² Shelley Hay,¹ Vasilios Liapis,¹ Irene Zinonos,¹ Natalie A. Sims,³ Gerald J. Atkins,¹ Cristina Vincent,¹ Vladimir Ponomarev,⁴ David M. Findlay,¹ Andrew C.W. Zannettino,² and Andreas Evdokiou¹

Abstract Purpose: Multiple myeloma is an incurable disease, for which the development of new therapeutic approaches is required. Here, we report on the efficacy of recombinant soluble Apo2L/tumor necrosis factor-related apoptosis-inducing ligand (TRAIL) to inhibit tumor progression and bone destruction in a xenogeneic model of human multiple myeloma.

Experimental Design: We established a mouse model of myeloma, in which Apo2L/TRAIL-sensitive RPMI-8226 or KMS-11 cells, tagged with a triple reporter gene construct (NES-HSV-TK/GFP/Luc), were transplanted directly into the tibial marrow cavity of nude mice. Tumor burden was monitored progressively by bioluminescence imaging and the development of myeloma-induced osteolysis was measured using high resolution *in vivo* micro-computed tomography.

Results: Tumor burden increased progressively in the tibial marrow cavity of mice transplanted with Apo2L/TRAIL-sensitive RPMI-8226 or KMS-11 cells associated with extensive osteolysis directly in the area of cancer cell transplantation. Treatment of mice with recombinant soluble Apo2L/TRAIL reduced myeloma burden in the bone marrow cavity and significantly protected against myeloma-induced osteolysis. The protective effects of Apo2L/TRAIL treatment on bone were mediated by the direct apoptotic actions of Apo2L/TRAIL on myeloma cells within the bone microenvironment.

Conclusions: This is the first *in vivo* study that investigates the efficacy of recombinant Apo2L/TRAIL on myeloma burden within the bone microenvironment and associated myeloma-induced bone destruction. Our findings that recombinant soluble Apo2L/TRAIL reduces myeloma burden within the bone microenvironment and protects the bone from myeloma-induced bone destruction argue against an inhibitory role of osteoprotegerin in Apo2L/TRAIL-induced apoptosis *in vivo* and highlight the need to clinically evaluate Apo2L/TRAIL in patients with multiple myeloma.

Multiple myeloma is a B-cell malignancy characterized by the presence of a monoclonal population of plasma cells, which localize to sites in the bone marrow close to the endosteal surface (1). Multiple myeloma is unique among hematologic

malignancies in its capacity to cause massive osteoclast-mediated destruction throughout the axial and craniofacial skeleton. The focal osteolytic lesions result in a range of debilitating clinical symptoms including bone pain, pathologic fractures, spinal cord compression, hypercalcemia, and renal failure (2). Although the precise mechanisms remain to be determined, numerous studies show that multiple myeloma plasma cells stimulate focal bone loss by promoting the aberrant recruitment and activation of osteoclast precursors from the peripheral blood to the endosteal and trabecular bone surfaces in close proximity to nests of multiple myeloma plasma cells and also inhibit osteoblastic bone formation [refs. 3, 4 and reviewed by Heider et al. (5)]. Despite many recent advances in clinical therapy, multiple myeloma remains an incurable disease, necessitating the development of new and safe therapeutic approaches.

Apo2 ligand/tumor necrosis factor-related apoptosis-inducing ligand (TRAIL) represents a promising new candidate drug for the treatment of multiple myeloma. Apo2L/TRAIL induces apoptosis in a variety of tumor cell types via interactions with its death domain-containing receptors DR4 and DR5 to activate caspases that carry out the cell death program. Three homologous human decoy receptors for Apo2L/TRAIL have also

Authors' Affiliations: ¹Discipline of Orthopaedics and Trauma, The University of Adelaide, Royal Adelaide Hospital, and Hanson Institute; ²Myeloma and Mesenchymal Research Laboratory, Bone and Cancer Laboratories, Division of Haematology, Institute of Medical and Veterinary Science, and Hanson Institute, Adelaide, South Australia, Australia; ³St. Vincent's Institute of Medical Research, Fitzroy, Victoria, Australia; and ⁴Department of Neurology, Memorial Sloan-Kettering Cancer Center, New York, New York

Received 9/22/08; revised 10/29/08; accepted 11/25/08; published OnlineFirst 3/10/09.

Grant support: National Health and Medical Research Council of Australia, The Cancer Council of South Australia, and National Breast Cancer Foundation.

The costs of publication of this article were defrayed in part by the payment of page charges. This article must therefore be hereby marked *advertisement* in accordance with 18 U.S.C. Section 1734 solely to indicate this fact.

Note: A.C.W. Zannettino and A. Evdokiou are considered equal senior authors.

Requests for reprints: Andreas Evdokiou, Discipline of Orthopaedics and Trauma, The University of Adelaide, Royal Adelaide Hospital, and Hanson Institute, Level 4, Bice Building, North Terrace, Adelaide 5000, South Australia, Australia. Phone: 61-8-82223107; Fax: 61-8-82323065; E-mail: andreas.evdokiou@adelaide.edu.au.

©2009 American Association for Cancer Research.

doi:10.1158/1078-0432.CCR-08-2444

Translational Relevance

Multiple myeloma is an incurable disease, for which the development of new therapeutic approaches is required. Here, we report for the first time on the efficacy of recombinant soluble Apo2L/tumor necrosis factor-related apoptosis-inducing ligand (TRAIL) to inhibit tumor progression and bone destruction in a xenogeneic model of human multiple myeloma. Previous studies have raised the possibility that the activity of soluble Apo2L/TRAIL may be abrogated in the bone microenvironment, where expression of the antagonistic decoy receptor for Apo2L/TRAIL, osteoprotegerin, is high, and speculated that recombinant soluble Apo2L/TRAIL may have limited use as a therapeutic agent for the treatment of skeletal malignancies. Our findings that recombinant soluble Apo2L/TRAIL reduces myeloma burden within the bone microenvironment and protects the bone from myeloma-induced bone destruction argue against an inhibitory role of osteoprotegerin in Apo2L/TRAIL-induced apoptosis *in vivo* and highlight the need to clinically evaluate Apo2L/TRAIL in patients with multiple myeloma. Given its imminent use in the clinic, we strongly feel that the antimyeloma activity of the only available clinical grade of recombinant soluble Apo2L/TRAIL should be reported.

been identified, including DcR1, DcR2, and osteoprotegerin (OPG; refs. 6, 7). Whereas DR4 and DR5 contain cytoplasmic death domains and on ligation induce apoptosis in Apo2L/TRAIL-sensitive cells, DcR1 and DcR2 lack functional death domains and cannot mediate apoptosis. OPG is a widely expressed soluble member of the tumor necrosis factor receptor family that is capable of binding to Apo2L/TRAIL, and although it has lower affinity for Apo2L/TRAIL at normal physiologic temperature, it can block Apo2L/TRAIL-induced apoptosis *in vitro* (8–11). Although other apoptosis-inducing members of the tumor necrosis factor family, such as tumor necrosis factor- α and Fas ligand, initially carried great promise as anticancer agents, their severe toxicity toward normal tissues precluded their clinical use. In contrast, Apo2L/TRAIL is selectively toxic to cancer cells and exhibits no toxicity to normal cells (12, 13). For example, our previous studies have shown that normal human bone cells, normal mammary epithelial cells, and human fibroblasts are resistant to Apo2L/TRAIL-induced apoptosis *in vitro* despite constitutive expression of Apo2L/TRAIL and its death receptors (14, 15). Although the mechanisms underlying the differential sensitivity to Apo2L/TRAIL of different tumor types or between tumors of the same type remain to be fully elucidated, multiple mechanisms appear to be involved. These include increased expression of the decoy receptors for Apo2L/TRAIL (16–20) and the overexpression of intracellular inhibitory proteins such as FLIP (16) or intracellular inhibitor of apoptosis molecules (21).

The antitumor activity of Apo2L/TRAIL has been well demonstrated in several mouse xenograft models of human soft tissue cancers, including colorectal (22), breast (12), lung (23), and glioma (24). Apo2L/TRAIL was active as a single agent and exhibited synergistic activity with certain chemo-

therapeutic agents or radiotherapy, causing marked regression or complete remission of tumors, with no evidence of toxicity to normal tissues and organs of the animals (25, 26). Phase Ia clinical trials of soluble, recombinant Apo2L/TRAIL in patients with a variety of solid tumor types and non-Hodgkin's lymphoma have shown that Apo2L/TRAIL is safe and well tolerated (27). Preliminary results in six low-grade non-Hodgkin's lymphomas, previously treated with rituximab, revealed that this particular combination with Apo2L/TRAIL was well tolerated and induced complete remission in two patients and partial remission or stable disease in another three patients (28). Further dose optimization is currently under way. In the context of multiple myeloma, previous studies have shown that Apo2L/TRAIL induces apoptosis of myeloma cells *in vitro* and reduces tumor burden in subcutaneous models of myeloma growth *in vivo* (8, 10, 29). However, the efficacy of Apo2L/TRAIL on myeloma burden in bone and myeloma-induced bone destruction has not been investigated. We have recently shown that recombinant soluble Apo2L/TRAIL prevents breast cancer-induced bone destruction in a mouse model by directly targeting cancer cells within the bone microenvironment and with no evidence of toxic side effects to normal tissues and organs. This work highlighted the potential for Apo2L/TRAIL therapy against bone-related malignancies.

Previous studies have raised the possibility that the activity of soluble Apo2L/TRAIL may be abrogated in the bone microenvironment, where expression of the antagonistic decoy receptor for Apo2L/TRAIL, OPG, is high and speculated that recombinant soluble Apo2L/TRAIL may have limited use as a therapeutic agent for the treatment of skeletal malignancies (8, 10, 11). To examine the antimyeloma activity of Apo2L/TRAIL within bone, we established a mouse model in which Apo2L/TRAIL-sensitive RPMI-8226 multiple myeloma or KMS-11 cells, tagged with a triple reporter gene construct (NES-HSV-TK/GFP/Luc; ref. 30), were transplanted directly into the tibial marrow cavity of nude mice. The intratibial injection model results in the formation of focal osteolytic lesions, which are localized to a single bony site and produce a consistent measurable outcome, enabling assessment of the efficacy of Apo2L/TRAIL treatment. An added advantage of this model is that the contralateral tibia in the same animal can be used as a control. This allows evaluation of the effects of treatment on myeloma burden and myeloma-induced osteolysis as well as the effects of Apo2L/TRAIL treatment on normal bone metabolism by comparing the non-tumor-bearing bones of the treated and vehicle-treated groups. Our findings that recombinant soluble Apo2L/TRAIL reduces myeloma burden within the bone microenvironment and protects the bone from myeloma-induced bone destruction argue against an inhibitory role of OPG in Apo2L/TRAIL-induced apoptosis *in vivo* and highlight the need to clinically evaluate recombinant soluble Apo2L/TRAIL in patients with multiple myeloma.

Materials and Methods

Cells and reagents

The human multiple myeloma cell lines WL2, ARH-77, U266, RPMI-8226, KMS-11, LP-1, and NCI-929 were obtained from the American Type Culture Collection and cultured in DMEM, supplemented with glutamine

(2 mmol/L), penicillin (100 IU/mL), streptomycin (100 µg/mL), gentamicin (160 µg/mL), and 10% fetal bovine serum (Biosciences), in a humidified atmosphere containing 5% CO₂. Recombinant soluble Apo2L/TRAIL was a gift from Dr. Avi Ashkenazi (Genentech). Zoledronic acid was generously provided by Novartis Pharma. The tetrapeptide caspase inhibitor zVAD-fmk was purchased from Calbiochem.

Measurement of cell viability

For determination of Apo2L/TRAIL effects on cell growth, 1×10^4 cells per well were seeded in 96-well microtiter plates. The following day, fresh medium containing increasing concentrations of Apo2L/TRAIL (3-300 ng/mL) was added for 24 h. Cell viability was determined using the WST-1 cell proliferation reagent assay kit (Roche Molecular Biochemicals). The absorbance was measured at 420 to 480 nm using an ELISA plate reader. Experiments comprised quadruplicate determinations and experiments were repeated at least three times. Results of experiments are given as the mean \pm SD.

Apoptosis analysis

4,6-Diamidino-2-phenylindole staining of nuclei. Cells were seeded on plastic chamber slides and treated as indicated. After two washes with PBS, cells were fixed in methanol for 5 min, washed again with PBS, and incubated with 0.8 mg/mL 4',6-diamidino-2-phenylindole (Roche Diagnostics) in PBS for 15 min at 37°C. After several washes in PBS, the coverslips were mounted on PBS/glycerol. 4',6-Diamidino-2-phenylindole staining was visualized by fluorescence microscopy.

Measurement of DEVD-caspase activity. DEVD-caspase activity was assayed by cleavage of zDEVD-AFC, a fluorogenic substrate based on the peptide sequence at the caspase-3 cleavage site of poly(ADP-ribose) polymerase. Cells (5×10^5) grown in 24-well plates were treated as indicated, washed once with HBSS, and resuspended in 200 µL NP-40 lysis buffer containing 5 mmol/L Tris-HCl, 5 mmol/L EDTA, and 0.5% NP-40 (pH 7.5). Cell lysate (20 µL) was added to each assay tube containing 8 µmol/L substrate in 1 mL protease buffer [50 mmol/L HEPES, 10% sucrose, 10 mmol/L DTT, 0.1% CHAPS (pH 7.4)]. After 4 h at room temperature, fluorescence was quantified (Ex 400 and Em 505) in a Perkin-Elmer LS50 fluorescence spectrometer. Optimal amounts of added lysate and duration of assay were taken from linear portions of curves as determined in preliminary experiments.

Western blot analysis

Primary antibodies were purchased from Chemicon International (polyclonal antibody anti-bid), Pharmingen International (polyclonal antibody anti-caspase-8), Cell Signaling Technology (polyclonal antibody anti-caspase-9), Medical and Biological Laboratories [monoclonal antibody (mAb) anti-caspase-10], Transduction Laboratories (mAb anti-caspase-3), and Roche Diagnostics [polyclonal antibody anti-poly(ADP-ribose) polymerase]. Anti-actin polyclonal antibody (Santa Cruz Biotechnology) was used to normalize for protein concentration. Membranes were rinsed several times with PBS containing 0.1% Tween 20 and incubated with 1:5,000 dilution of anti-mouse or anti-rabbit alkaline phosphatase-conjugated secondary antibodies (Amersham) for 1 h. Visualization and quantification of protein bands were done using the Vistra ECF substrate reagent kit (Amersham) on a FluorImager (Molecular Dynamics).

Retroviral infection of RPMI-8226 and KMS-11 cells with the triple reporter gene construct SFG-NES-TGL

TK/GFP/Luc-expressing RPMI-8226 and KMS-11 cell lines were generated using the retroviral expression vector SFG-NES-TGL (30). Viral particle-containing supernatant was generated and filtered to remove any cellular debris and used to infect RPMI-8226 and KMS-11 cells as described previously (31). The retrovirally transduced cells were grown as bulk cultures for 48 h and subsequently sorted for positive green fluorescent protein (GFP) expression using fluorescence-activated cell sorting (Aria BD Biosciences). The cells were allowed to proliferate and the top 10% of GFP-expressing cells were sorted by fluorescence-

activated cell sorting to generate the sublines RPMI-8226-NES-TGL and KMS-11-TGL. To confirm luciferase expression, an *in vitro* bioluminescence assay was done. Bioluminescence was measured using Lumiscan Ascent and analyzed by Ascent software (ThermoFisher Scientific).

Animals

Female athymic nude mice at age 4 to 6 weeks (Institute of Medical and Veterinary Science) were acclimatized to the animal housing facility for a minimum period of 1 week before the commencement of experimentation. All of the experimental procedures on animals were carried out with strict adherence to the rules and guidelines for the ethical use of animals in research and were approved by the Animal Ethics Committee of the Institute of Medical and Veterinary Science.

Intratumoral implantation of multiple myeloma cells

Multiple myeloma RPMI-8226-NES-TGL or KMS-11-TGL cells were inoculated intratumorally as described previously (32, 33). Cells in log-phase growth were aspirated into a 25 µL Hamilton syringe (Alltech Associates) coupled to a 27-gauge needle. The needle was inserted through the cortex of the anterior tuberosity of the left tibia. Once the bone cortex was traversed, the needle was inserted 3 to 5 mm down the diaphysis of the tibia, and 10 µL of the cell suspension (1×10^6 cells per inoculum) were injected into the marrow space. The right contralateral tibia was injected with PBS alone as an internal control. For each of the two independent experiments in which RPMI-8226-TGL cells were injected intratumorally, mice were randomized into two groups of 10 mice per group. Two days after cancer cell transplantation, Apo2L/TRAIL was administered (intraperitoneally) at 30 mg/kg/dose once per day for 5 consecutive days followed by a once weekly dose until termination of the experiment. The control group was given PBS administered intraperitoneally. Mice from experiments 1 and 2 were humanely killed at 5 weeks after cancer cell implantation. In a parallel, experiment mice ($n = 10$) were injected subcutaneously with the antiresorptive bisphosphonate zoledronic acid (Novartis Pharma) at 100 µg/kg/dose once weekly for 5 weeks as a positive control for comparison. Animals transplanted with KMS-11 cells were left untreated until tumors became well established and Apo2L/TRAIL was administered on day 21 (intraperitoneally) at 30 mg/kg/dose once per day for 5 consecutive days followed by a once weekly dose until termination of the experiment on day 42.

In vivo bioluminescent imaging

Noninvasive, whole-body imaging to monitor luciferase-expressing RPMI-8226-NES-SFG-TGL or KMS-11-TGL cells in mice was done weekly using the IVIS 100 Imaging System (Xenogen). About 30 min before analysis, mice were injected intraperitoneally with 100 µL D-luciferin solution at 250 mg/kg body weight (Xenogen) and then gas-anesthetized with isoflurane (Faulding Pharmaceuticals). Images were acquired for 0.5 to 10 s and the photon emission transmitted from mice was captured and quantitated in photons/s/cm²/sr using Xenogen Living image (Igor Pro version 2.5) software.

Micro-computed tomography analysis

In vivo live micro-computed tomography imaging. Computed tomography (CT) images were obtained using a Skyscan-1076 *in vivo* micro-CT scanner (Skyscan) at fortnightly intervals while the animals were anesthetized. The micro-CT scanner was operated at 80 kV, 120 µA, rotation step 0.5, 0.5 mm Al filter, scan resolution of 17.4 µm/pixel, and imaging time of 15 min. The cross-sections were reconstructed using a cone-beam algorithm (software Cone_rec; Skyscan). Files were then imported into CTAn software (Skyscan) for three-dimensional analysis and three-dimensional image generation. All images are viewed and edited using ANT visualization software.

Ex vivo micro-CT imaging. Limbs for micro-CT analysis were surgically resected and scanned using the Skyscan-1072 high-resolution micro-CT scanner (Skyscan). The micro-CT scanner was operated at 80 kV, 120 µA, rotation step 0.675, 0.5 mm Al filter, and scan resolution

of 5.2 $\mu\text{m}/\text{pixel}$. Using the two-dimensional images obtained from the micro-CT scan, the growth plate was identified and 750 sections were selected starting from the growth plate/tibial interface and moving down the tibia. For quantification, three-dimensional evaluation was done on all data sets acquired by selecting two separate regions of interest, one for total bone and another containing the trabecular spongiosa of the proximal tibia only, to determine three-dimensional bone morphometric parameters (software CTAn; Skyscan).

Histology

Tibiae were fixed in 10% (v/v) buffered formalin (24 h at 4°C) followed by 2 weeks of decalcification in 0.5 mol/L EDTA/0.5% paraformaldehyde in PBS (pH 8.0) at 4°C. Complete decalcification was confirmed by radiography and tibiae were then paraffin embedded. Longitudinal sections (5 μm) were prepared and stained with H&E. The same sections were used for TUNEL staining using the ApopTag Plus *in situ* apoptosis detection kit (Chemicon International) as per manufacturer's instructions. Analysis was done on an Olympus CX41 microscope.

Isolation of tumors or explants from the bone marrow of tibia

Tibiae were cut below the growth plate and above the feet and a 25-gauge needle was used to flush cells from the bone marrow cavity with PBS. The *ex vivo* cells were sorted by fluorescence-activated cell sorting to isolate the highly GFP-expressing cells designated here as RPMI-8226-NES-TGL-*ex vivo* and seeded into 96-well plates before treatment with 100 ng/mL Apo2L/TRAIL to examine changes in drug sensitivity.

Generation of Apo2L/TRAIL-resistant RPMI-8226-NES-TGL cells *in vitro*

RPMI-8226-NES-TGL cells were seeded in a T75 flask until 75% confluence. Cells were exposed to Apo2L/TRAIL at 25 ng/mL for the first 2 weeks, at which time the concentration of Apo2L/TRAIL was increased to 50 ng/mL for a further 2 weeks followed by treatment in 100 ng/mL for a further 4 weeks. During the selection period, cell debris was removed every 3 days and cells were incubated with fresh medium containing Apo2L/TRAIL for 8 weeks. Thereafter, Apo2L/TRAIL-resistant cells, denoted RPMI-8226-NES-TGL-R, were cultured in Apo2L/TRAIL-free medium and were found to remain resistant.

Cell surface expression of DR4 and DR5

For each of the cell lines RPMI-8226-NES-TGL, RPMI-8226-NES-TGL-R, and RPMI-8226-NES-TGL-*ex vivo*, cells were collected, washed in 1% bovine serum albumin and 0.1% sodium azide in PBS, and resuspended in 50 μL blocking buffer (5% normal goat serum, 1% bovine serum albumin in PBS + 0.1% sodium azide) on ice. mAb against TRAIL-R1/DR4 (IgG1, MAB347) was purchased from R&D Systems, whereas monoclonal antibodies against TRAIL-R2/DR5 (IgG1, M413), TRAIL-R3/DcR1 (IgG1, M430), and TRAIL-R4/DcR2 (IgG1, M444) were kindly supplied by Amgen. The mAb 1B5 was used as the IgG1 isotype control. Antibodies were added to cells at 20 $\mu\text{g}/\text{mL}$ and left for 1 h on ice. Cells were washed and the secondary antibody was added ($\alpha\text{IgG-PE}$; Southern Biotech) and left on ice for a further 45 min. Cells were washed and resuspended in fluorescence-activated cell sorting fix until analysis by flow cytometry.

Histomorphometric analysis

To determine the effects of Apo2L/TRAIL on normal bone morphometry, fixed tibiae were embedded in methylmethacrylate (34, 35) and 5 μm sections were stained with toluidine blue (35). Histomorphometry was carried out in the secondary spongiosa of the proximal tibia (osteomeasure; Osteometrics) as described previously (35).

Data analysis and statistics

Experiments were done in triplicate, and data are presented as mean \pm SE. All statistical analysis was done using SigmaStat for Windows version 3.0 (Systat Software) using the unpaired Student's *t* test. Measures of association between two variables were assessed using the Spearman rank correlation coefficient. Comparisons between groups were assessed using a one-way ANOVA test. In all cases, $P < 0.05$ was considered statistically significant.

Results

Effect of Apo2L/TRAIL on multiple myeloma cells *in vitro*. A panel of seven well-established human multiple myeloma cell lines were examined for their sensitivity to the cytotoxic effects of Apo2L/TRAIL. As shown in Fig. 1A, only RPMI-8226 and KMS-11 exhibited a dose-dependent loss of cell viability after treatment for 24 h, reaching a maximum of 80% loss of viability at the highest dose of 300 ng/mL Apo2L/TRAIL (Fig. 1A). The remaining cell lines were relatively resistant to the effects of Apo2L/TRAIL. Treatment of RPMI-8226 cells with Apo2L/TRAIL induced morphologic changes characteristic of apoptosis, including chromatin condensation and DNA fragmentation (Fig. 1B) and a dose-dependent activation of caspase-3, which reached maximum at 25 ng/mL and plateaued thereafter (Fig. 1C). The presence of a pan-caspase inhibitor, zVAD-fmk, completely reversed the reduction in cell viability induced by Apo2L/TRAIL (Fig. 1C). Apoptosis induction was associated with processing and activation of the initiator caspase-8 and caspase-10, leading to cleavage pro-caspase-3, which was concomitant with cleavage of the apoptosis target protein poly(ADP-ribose) polymerase (Fig. 1D). Activation of the intrinsic apoptotic pathway was associated with caspase-8-mediated cleavage of the Bcl-2 protein family member Bid and activation of caspase-9. Similar effects were also seen with KMS-11 cells (data not shown).

Antitumor activity of Apo2L/TRAIL in a mouse model of multiple myeloma. To evaluate the efficacy of recombinant soluble Apo2L/TRAIL to inhibit tumor growth and bone destruction, we established a xenogeneic tumor model of human multiple myeloma, in which the Apo2L/TRAIL-sensitive RPMI-8226 cells were transplanted directly into the marrow tibial cavity of athymic nude mice. For noninvasive bioluminescence imaging (BLI) of tumor growth, the parental cells were retrovirally infected with a triple-fusion protein reporter construct encoding HSV-TK/GFP/Luc (30). After infection, the myeloma cells were enriched for high-level expression of GFP by two rounds of fluorescence-activated cell sorting, thus generating the subline RPMI-8226-NES-TGL. The selected cells exhibited a 1,000-fold induction of luciferase activity when analyzed *in vitro*. When compared with the parental noninfected myeloma cells, RPMI-8226-NES-TGL cells were equally responsive to Apo2L/TRAIL, with both lines showing high sensitivity to the apoptotic effects of the ligand and with similar kinetics of caspase-3 activity (Fig. 1E). RPMI-8226-NES-TGL cells were injected within the left tibiae of mice and the right contralateral tibiae were injected with PBS. Tumor burden was assessed by weekly noninvasive BLI. Results from two separate animal experiments showed an exponential increase of photon emission associated with an increase in tumor burden, which was clearly evident from day 7 onwards in the untreated group of the first experiment and day 14 of the second experiment

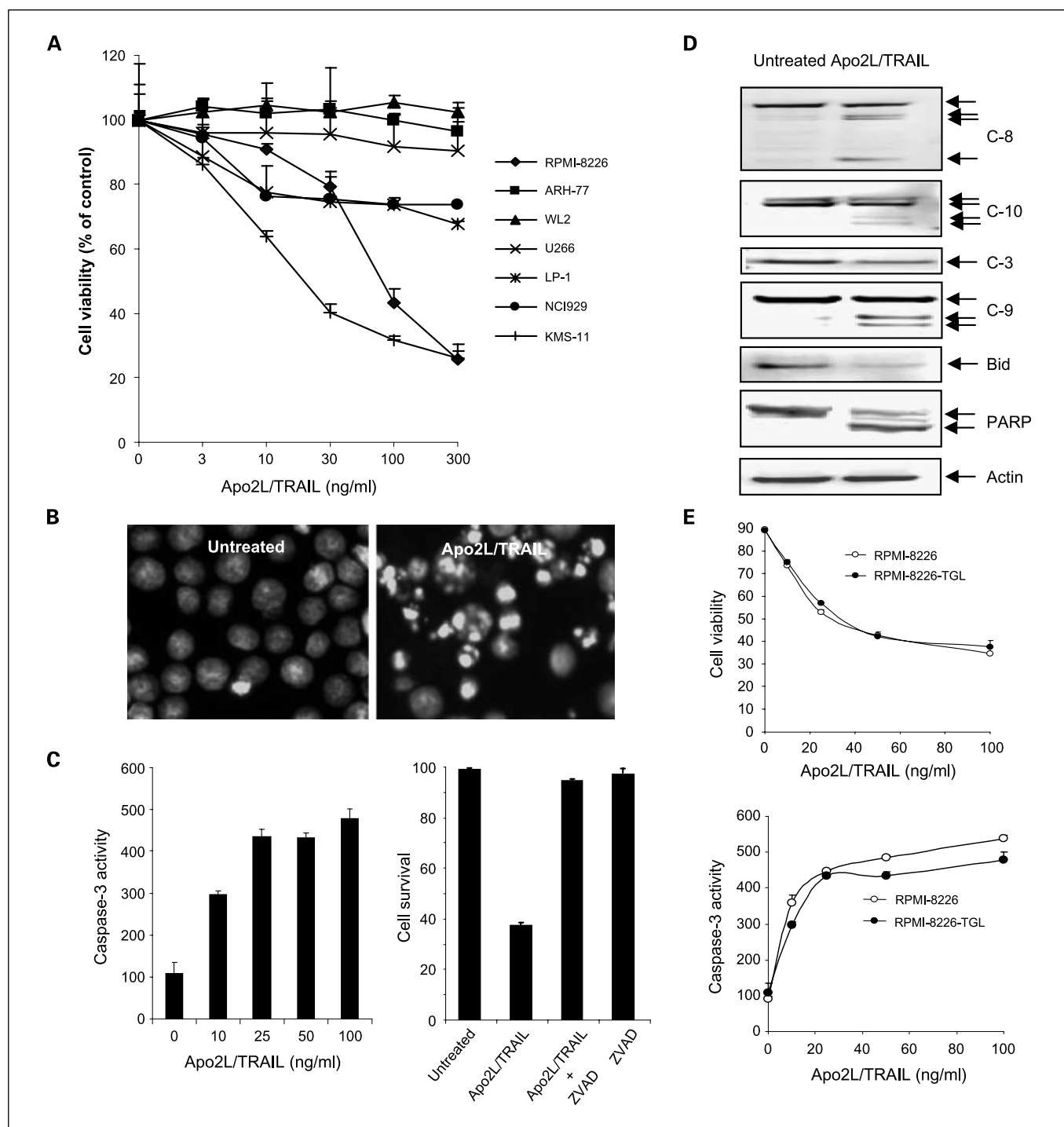


Fig. 1. Apo2L/TRAIL-induced apoptosis in multiple myeloma cell lines *in vitro*. **A**, comparison of the effect of Apo2L/TRAIL in a panel of well-established human multiple myeloma cell lines. Cells were left untreated or treated with increasing Apo2L/TRAIL concentrations of 3, 10, 30, 100, and 100 ng/mL and cell viability was determined by MTT assay 24 h thereafter. Representative experiment repeated at least three times. *Points*, mean; *bars*, SD. **B**, cells were seeded on chamber slides at 5×10^4 per chamber and treated with Apo2L/TRAIL at 100 ng/mL for 24 h. Cells were fixed with methanol and incubated with 4',6-diamidino-2-phenylindole before washing in PBS and mounting on PBS/glycerin. 4',6-Diamidino-2-phenylindole staining was visualized by fluorescence microscopy. **C**, *left*, RPMI-8226 cells were treated with Apo2L/TRAIL for 24 h. Cell lysates were used to determine caspase-3-like activity using the caspase-3 specific fluorogenic substrate, zDEVD-AFC, as described in Materials and Methods. *Right*, RPMI-8226 cells were treated for 24 h with 100 ng/mL Apo2L/TRAIL alone or coincubated with the broad-specificity caspase inhibitor zVAD-fmk (50 μ mol/L). To exclude possible toxic effects of the inhibitor, cells were also treated with the inhibitor alone. Cell viability was determined using the MTT assay and expressed as percentage of control. Quadruplicate results from a representative experiment repeated at least twice. *Points*, mean; *bars*, SD. **D**, RPMI-8226 cells were seeded at 2×10^6 per T25 flask and either left untreated or treated with Apo2L/TRAIL at a concentration of 100 ng/mL. Cells were then lysed and total cell lysates were analyzed by PAGE and transferred to polyvinylidene fluoride membranes for immunodetection. The caspase-8, caspase-9, caspase-10, and poly(ADP-ribose) polymerase antibodies detect both full-length and processed forms of the antigen, whereas caspase-3 and Bid antibodies detect only the full-length antigens. **E**, comparison of the effect of Apo2L/TRAIL on NES-HSV-TK/GFP/Luc retrovirally infected cells (RPMI-8226-NES-TGL) and their parental noninfected counterpart cells (RPMI-8226). Cells were left untreated or treated for 24 h with increasing concentrations Apo2L/TRAIL. Cell viability (*top*) and caspase-3 activity (*bottom*) were determined as described above. Representative experiments repeated at least three times. *Bars*, SD.

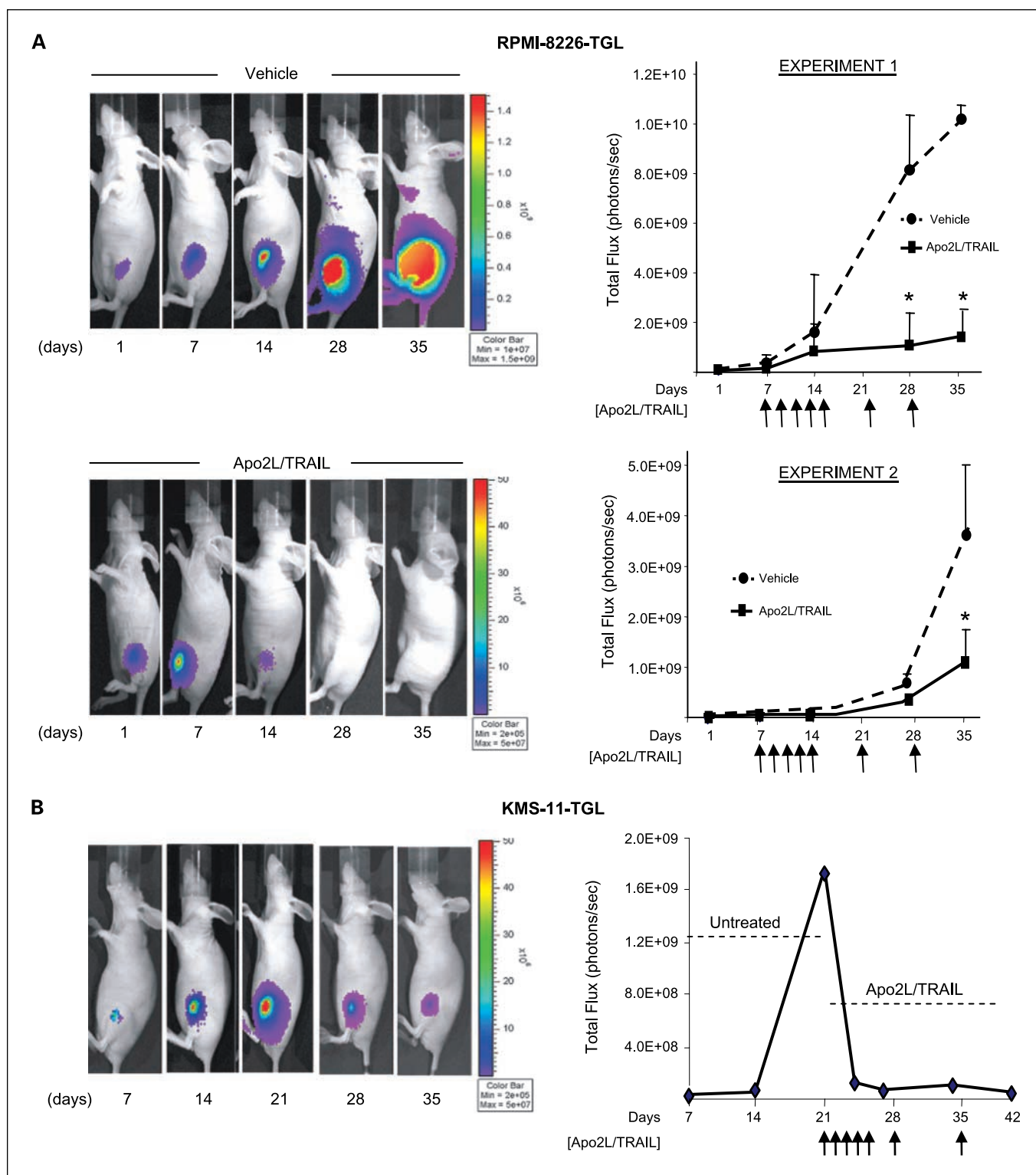


Fig. 2. Noninvasive *in vivo* BLI and quantification of the effect of Apo2L/TRAIL on multiple myeloma growth in the bone marrow. **A**, nude mice were injected with 1×10^6 RPMI-8226-NES-TGL cells into the left tibia, whereas the right contralateral tibia was injected with PBS alone as an internal control. Two independent experiments were carried out. For each experiment, mice were randomized into two groups of 10 mice per group. Seven days after cancer cell transplantation, Apo2L/TRAIL was administered (intraperitoneally) at 30 mg/kg/dose once per day for 5 consecutive days followed by a once weekly dose until termination of the experiment. Vehicle-treated animals received intraperitoneal injections of PBS adhering to the same schedule of Apo2L/TRAIL administration. **B**, nude mice ($n = 6$) were injected with 1×10^6 KMS-11-NES-TGL cells into the left tibia and tumors were allowed to progress to a define size as measured by photon counts per second. Apo2L/TRAIL was administered on day 21 after cancer cell transplantation once per day for 5 consecutive days followed by a once weekly dose. Mice were imaged weekly using the Xenogen IVIS 100 BLI system. Representative whole-body images of untreated and treated animals during the course of the experiments. BLI measurements are expressed as the sum of integrated photon counts per second. Mean \pm SE. A significant difference between the vehicle group and the Apo2L/TRAIL-treated group was observed on days 28 and 35 (* , $P < 0.01$) in experiment 1 and on day 35 in experiment 2 (* , $P < 0.05$).

(Fig. 2A). In contrast, animals treated intraperitoneally with 30 mg/kg/dose of Apo2L/TRAIL for 5 consecutive days, followed by once weekly injection for 6 weeks, exhibited a significant inhibition of tumor growth when compared with the vehicle-treated groups (Fig. 2A). We next assessed the tumor-suppressive activity of Apo2L/TRAIL against the only other sensitive myeloma cell line KMS-11-TGL. However, in this case, we allowed the tumors to establish and progress to a defined size with treatment initiated on day 21 after cancer cell transplantation. Treatment with Apo2L/TRAIL resulted in a significant regression of the tumors within the first week of treatment and bioluminescence signal was barely detectable thereafter (Fig. 2B). This indicates that this effect Apo2L/TRAIL was not cell line dependent but rather was a general

phenomenon. The effect of Apo2L/TRAIL on myeloma-induced osteolysis was assessed in detail with parallel qualitative assessment of bone architecture done in animals bearing RPMI-8226-TGL cells. Representative two-dimensional transversal and reconstructed three-dimensional live micro-CT images of the tumor-injected and contralateral non-tumor-injected tibiae of vehicle-treated animals revealed myeloma-induced osteolysis as early as day 14 followed by progressive severe bone destruction on days 28 and 35 following cancer cell transplantation (Fig. 3A). The focal and "punched out" osteolytic lesions resembled the lesions commonly seen in myeloma patients. In contrast, treatment with Apo2L/TRAIL resulted in a progressive reduction in myeloma-induced bone destruction. Although small osteolytic lesions were clearly

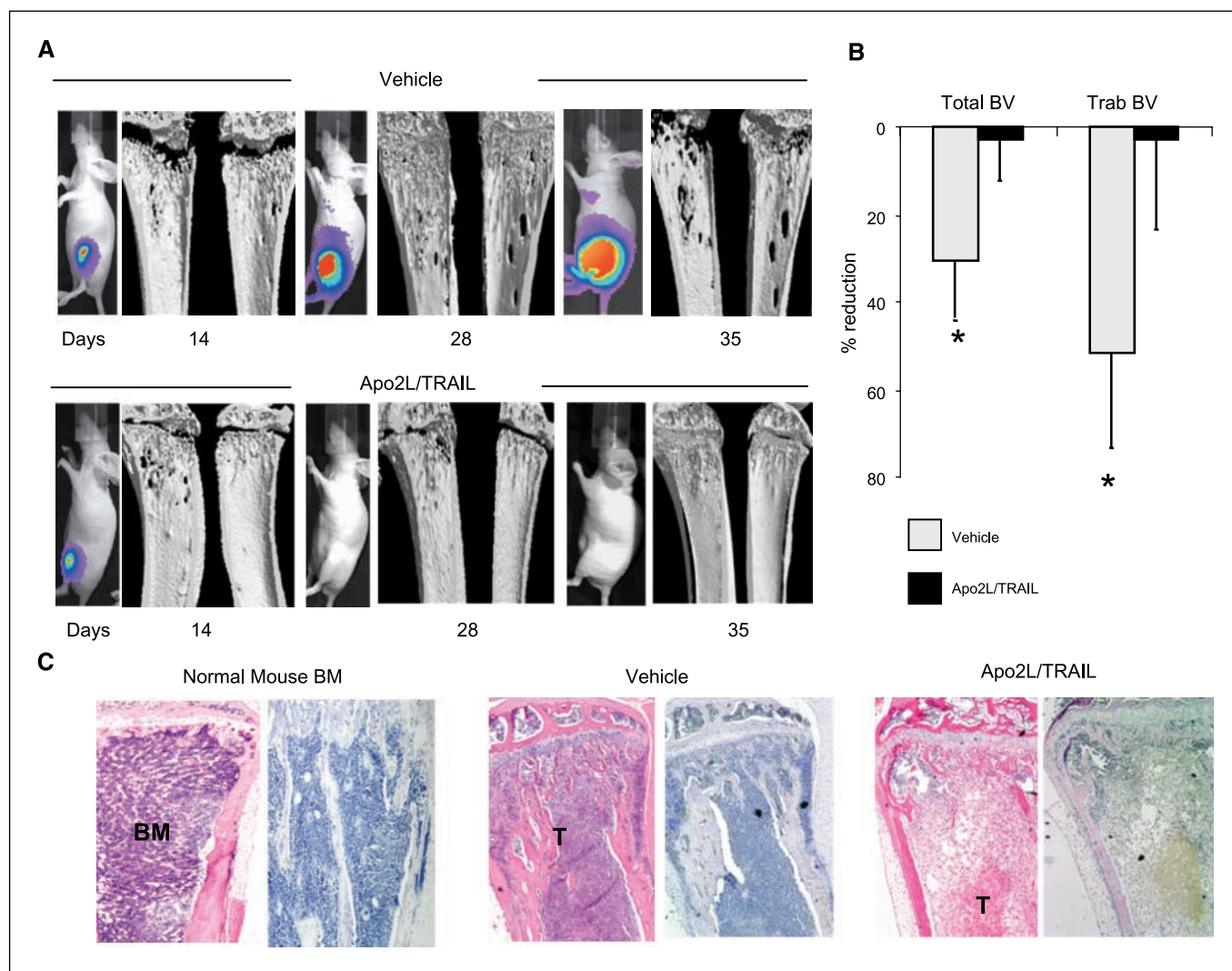


Fig. 3. Noninvasive *in vivo* micro-CT imaging and quantification of the effect of Apo2L/TRAIL on multiple myeloma-associated bone osteolysis. *A*, representative three-dimensional reconstructions of micro-CT images generated from serial two-dimensional cross-sectional micro-CT images (18 μ m resolution) covering the total length of each tumor-bearing tibiae taken on days 14, 28, and 42 after cancer cell transplantation. Progression of myeloma-induced osteolysis in the animals over time using *in vivo* micro-CT. Treatment with Apo2L/TRAIL resulted in a significant conservation of the tibiae concomitant with the reduction in myeloma burden in the marrow as assessed by BLI. *B*, bone morphometric parameters from tibiae of vehicle-treated ($n = 8$) or Apo2L/TRAIL-treated ($n = 8$) animals were quantified at the time of sacrifice using *ex vivo* high-resolution two-dimensional micro-CT images (5 μ m resolution) as described in Materials and Methods. The effect of Apo2L/TRAIL on total bone volume (*Total BV*) and trabecular bone volume (*Trab BV*) is expressed as the percentage reduction relative to mean value of vehicle-treated mice at end of the experiment (*, $P < 0.05$). *C*, representative H&E-stained decalcified tibial sections showing intense tunnel positive staining confirming the presence of apoptosis in a substantial fraction of the tumor (T) in the Apo2L/TRAIL-treated animals when compared with the tumor-bearing vehicle-treated animals or contralateral non-tumor-bearing tibia of Apo2L/TRAIL-treated animals, respectively.

evident on day 14, they did not progress further. Of interest, some of these lesions resolved with time, concomitant with reduction in tumor burden as assessed by BLI. The animals used in these studies were young, suggesting that the repair of these lesions is a result of rapid bone turnover. In addition to the qualitative assessment of osteolysis, morphometric parameters were quantified from the three-dimensional micro-CT data generated after termination of the experiments using the high-resolution desktop micro-CT (Fig. 3B). We compared the left tumor-bearing tibiae with the contralateral right non-tumor-bearing tibiae at a selected region beginning at the growth plate and extending downwards 750 micro-CT bone slices, each at a thickness of 5 μm . This region encompassed the osteolytic lesions. In the tumor-bearing tibiae of the untreated group, there was a significant decrease in trabecular bone volume and total bone volume when compared with the contralateral non-tumor-bearing tibiae of the same animals. Apo2L/TRAIL treatment showed that the myeloma-induced decrease in trabecular and total bone volume compared with the non-tumor-bearing tibiae was significantly reduced from 52% to 2.9% and 31% to 2.5%, respectively, clearly showing the protective effects of Apo2L/TRAIL treatment on myeloma-induced bone loss (Fig. 3B). Histologic examination of representative tibial sections from the untreated animals showed RPMI-8226-NES-TGL cells within the marrow cavity and in the surrounding soft tissue (Fig. 3C). Trabecular and cortical bone destruction was also evident, confirming the micro-CT data. In contrast, Apo2L/TRAIL treatment induced apoptosis in a substantial proportion of tumor cells, with intense positive TUNEL staining apparent only in the tumors of the Apo2L/TRAIL-treated animals but not in the vehicle-treated animals resulting in significantly smaller tumors that were in all cases confined within the marrow cavity. It was therefore evident that Apo2L/TRAIL treatment *in vivo* did not completely eradicate myeloma cells from the bone microenvironment. Residual myeloma cells were still evident among the necrotic tumor mass (Fig. 3C), suggesting that either schedule or dosing of Apo2L/TRAIL treatment was not 100% efficient and/or residual myeloma cells persisted within the bone marrow due to the development of Apo2L/TRAIL resistance with prolonged treatment *in vivo*. To examine these possibilities, the contents of the tibial marrow cavity were flushed out and the GFP-tagged myeloma cells were sorted by fluorescence-activated cell sorting and tested *in vitro* for their sensitivity to Apo2L/TRAIL. The myeloma cells (RPMI-8226-NES-TGL) flushed from the marrow cavity of animals that were never exposed to Apo2L/TRAIL remained highly sensitive to Apo2L/TRAIL-induced apoptosis, exhibiting 30% survival at a dose of 100 ng/mL Apo2L/TRAIL treatment for 24 h. In contrast, myeloma cells (RPMI-8226-NES-TGL-*ex vivo*) flushed from the Apo2L/TRAIL-treated animals showed increased resistance to the same dose of Apo2L/TRAIL, showing ~60% survival after treatment with the same dose of Apo2L/TRAIL *in vitro* (Fig. 4A). The decrease in Apo2L/TRAIL sensitivity was also reflected in the reduction in Apo2L/TRAIL-induced caspase-3 activity (Fig. 4A). These results suggest that the failure to completely eliminate myeloma cells from the marrow cavity may be due not only to inefficient death induction by Apo2L/TRAIL but also to the development of resistance leading to late recurrence. The latter is supported by our finding that continuous treatment *in vitro* of the highly sensitive RPMI-8226-NES-TGL cells with Apo2L/TRAIL led to

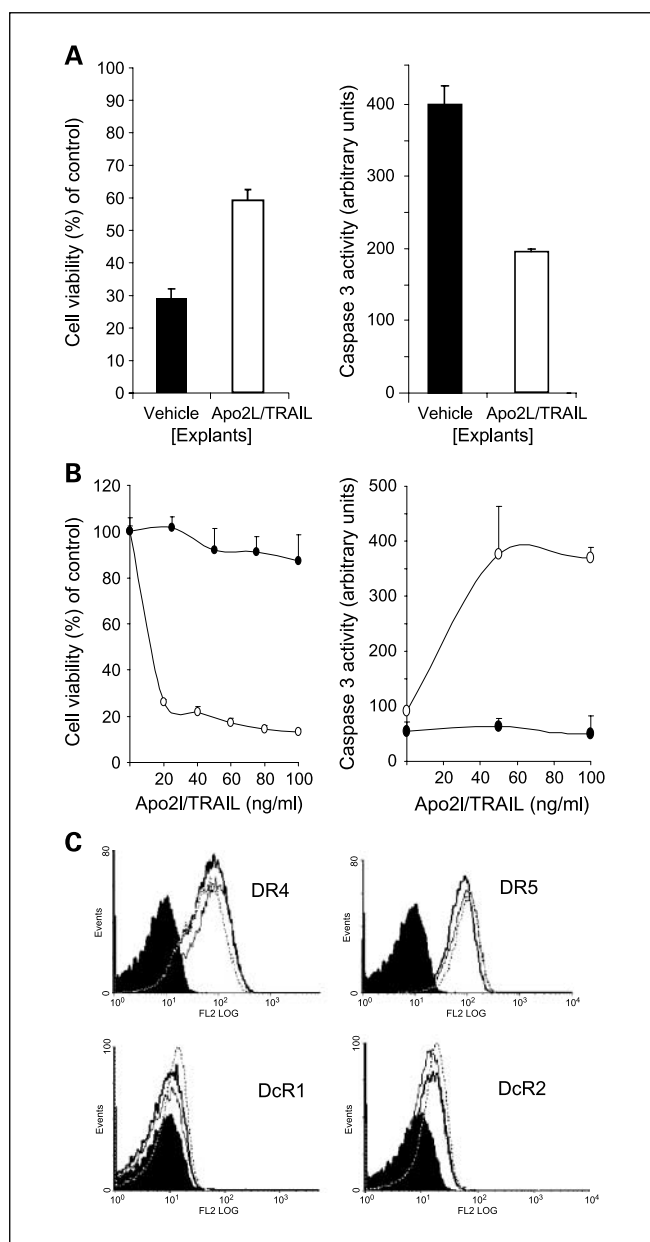


Fig. 4. Development of Apo2L/TRAIL resistance with prolonged treatment *in vivo* and *in vitro*. **A**, at the end of the experiment (day 42), RPMI-8226-NES-TGL cells were flushed from the tibiae of vehicle-treated (RPMI-8226-NES-TGL-vehicle) or Apo2L/TRAIL-treated (RPMI-8226-NES-TGL-Apo2L/TRAIL) animals and cultured *ex vivo* for 24 h in the presence of 100 ng/mL Apo2L/TRAIL. Cell viability was assessed by the MTT assay (*left*), whereas caspase-3 activity was measured from cell extracts isolated from the same cells as described in Materials and Methods (*right*). *Solid columns*, RPMI-8226-NES-TGL-vehicle cells; *empty columns*, RPMI-8226-NES-TGL-Apo2L/TRAIL. Average \pm SD of triplicates. $P < 0.05$. **B**, Apo2L/TRAIL-resistant cells were also generated *in vitro* by culturing the parental RPMI-8226-NES-TGL cells continuously in medium containing Apo2L/TRAIL for ~8 wk as described in Materials and Methods. These resistant cells (denoted RPMI-8226-NES-TGL-R), when compared with the parental cells (RPMI-8226-NES-TGL), were completely resistant to Apo2L/TRAIL, showing ~100% viability even at the highest dose of 100 ng/mL Apo2L/TRAIL (*left*) and showing lack of Apo2L/TRAIL-induced caspase-3 activity (*right*). **C**, flow cytometric analysis for cell surface expression of Apo2L/TRAIL receptors in the parental sensitive RPMI-8226-NES-TGL cells (*dark solid line*), resistant RPMI-8226-NES-TGL-R cells (*dotted line*), and intermediately sensitive RPMI-8226-NES-TGL-Apo2L/TRAIL cells (*light solid line*). Depicted graphs were obtained after staining with anti human TRAIL/DR4, TRAIL/DR5, TRAIL/DcR1, and TRAIL/DcR2 monoclonal antibodies as described in Materials and Methods. *Shaded curves*, isotype control staining with the IB5 IgG1 mAb; *unshaded curves*, staining with the respective Apo2L/TRAIL receptor antibodies.

Table 1. Bone histomorphometric analysis of vehicle-treated and Apo2L/TRAIL-treated animals

Parameters	Vehicle control (n = 6)	Apo2L/TRAIL (n = 6)	P
Trabecular bone volume (%)	2.00 ± 0.76	2.82 ± 1.22	0.59
Trabecular number (1/mm)	24.69 ± 3.20	28.80 ± 0.84	0.26
Trabecular spacing (mm)	1,873 ± 617	1,831 ± 830	0.97
Trabecular thickness (1/mm)	0.73 ± 0.22	1.01 ± 0.90	0.60
Bone volume occupied by osteoid (%)	4.30 ± 1.82	1.57 ± 0.90	0.23
Osteoid surface (%)	15.43 ± 5.83	6.15 ± 2.97	0.21
Osteoblast surface (%)	15.16 ± 5.90	6.63 ± 3.11	0.25
No. osteoblast/bone perimeter (#/mm)	9.30 ± 3.47	3.94 ± 1.80	0.22
Osteoclast surface (%)	6.46 ± 1.93	3.21 ± 0.55	0.16

NOTE: Value in table expressed as mean ± SE.

the development of resistant clones (RPMI-8226-NES-TGL-R) that were completely refractory to the apoptotic effects of the ligand and showed no detectable Apo2L/TRAIL-induced caspase-3 activation when compared with the parental cells (Fig. 4B). To investigate the reason for the development of Apo2L/TRAIL resistance *in vitro*, we compared the expression profile of Apo2L/TRAIL receptors between sensitive and resistant cells using flow cytometric analysis to detect cell surface expression of the receptors (Fig. 4C). The parental (sensitive) RPMI-8226-NES-TGL cells expressed high levels of DR4 and DR5 on the cell surface but low levels of DcR1 and DcR2. Furthermore, this pattern of cell surface receptor expression was not altered in either RPMI-8226-NES-TGL-R or RPMI-8226-NES-TGL-*ex vivo* cells, suggesting that in this case death receptor levels are not predictive of Apo2L/TRAIL sensitivity (Fig. 4C).

Effect of Apo2L/TRAIL on normal bone metabolism. Recent work by Zauli et al. showed that injection of mice with soluble Apo2L/TRAIL induced a significant increase in tibial trabecular thickness and total bone mass, suggesting that Apo2L/TRAIL may regulate normal bone metabolism via inhibition of host osteoclast differentiation and bone resorption (36). To assess the effect of Apo2L/TRAIL treatment on normal bone remodeling, we performed histomorphometry on the contralateral non-tumor-bearing tibiae from the Apo2L/TRAIL-treated animals

and compared these with the untreated group. The effect of Apo2L/TRAIL treatment on indices of bone resorption and formation, including osteoclast surface, osteoblast surface, osteoid volume, and osteoid surface, as well as bone structural parameters, including trabecular bone volume, trabecular number, trabecular thickness, and trabecular spacing, was not significantly different compared with untreated animals (Table 1). In a different cohort of control animals, the effect of Apo2L/TRAIL treatment was assessed in parallel with the bisphosphonate zoledronic acid by three-dimensional micro-CT analysis. As anticipated, treatment with zoledronic acid induced a profound and highly significant increase in all morphometric parameters, including total bone volume and trabecular volume, with respect to vehicle-treated animals (Table 2). These data were consistent with the qualitative assessment of bone architecture as depicted from three-dimensional micro-CT scans (Fig. 5). In contrast, no significant changes in any parameters were detected with Apo2L/TRAIL treatment, confirming the histomorphometric data.

Discussion

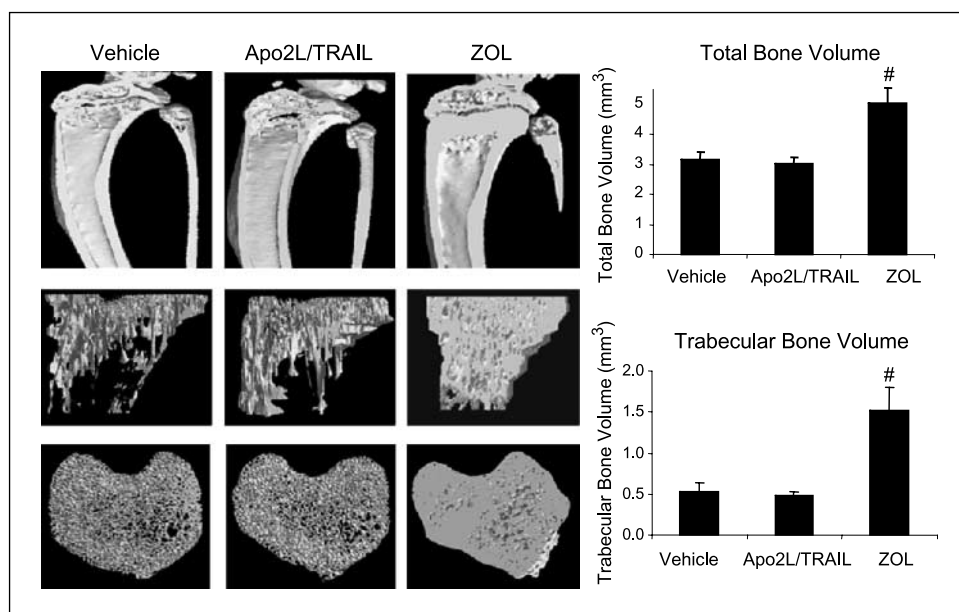
Previous studies have shown that Apo2L/TRAIL induces apoptosis of myeloma cells *in vitro* and reduces tumor burden in subcutaneous models of myeloma growth *in vivo* (10, 29).

Table 2. Comparison of bone morphometric parameters of contralateral non-tumor-injected tibiae from untreated, Apo2L/TRAIL-treated, or zoledronic acid-treated animals

Parameters	Vehicle control	Apo2L/TRAIL		ZOL	
	Mean ± SE	Mean ± SE	P	Mean ± SE	P
Total bone volume (mm ³)	3.16 ± 0.10	2.94 ± 0.08	0.13	5.02 ± 0.22	<0.01
Trabecular bone volume (mm ³)	0.53 ± 0.05	0.48 ± 0.02	0.39	1.54 ± 0.11	<0.01
Bone surface/bone volume ratio (1/mm)	94.36 ± 1.99	90.94 ± 2.12	0.30	63.97 ± 2.39	<0.01
Bone surface (mm ²)	49.15 ± 3.95	43.65 ± 0.90	0.20	95.98 ± 5.38	<0.01
Intersection surface (mm ²)	3.97 ± 0.29	3.60 ± 0.24	0.35	7.51 ± 0.29	<0.01
Trabecular space (mm)	0.34 ± 0.03	0.33 ± 0.01	0.60	0.19 ± 0.01	<0.01
Trabecular number (1/mm)	4.43 ± 0.20	4.30 ± 0.13	0.52	9.60 ± 0.44	0.03
Trabecular thickness (1/mm)	0.05 ± 0.00	0.05 ± 0.00	0.69	0.05 ± 0.00	<0.01
Trabecular pattern factor (1/mm)	-5.89 ± 0.64	0.74 ± 1.21	0.54	-88.80 ± 5.67	<0.01
Structure model index	1.60 ± 0.06	1.65 ± 0.06	0.58	-2.76 ± 0.37	<0.01

NOTE: Total bone volume, trabecular bone volume, bone surface to bone volume ratio, bone surface, intersection surface, trabecular space, trabecular number, trabecular thickness, trabecular pattern factor, and structure model index were measured by three-dimensional analysis of micro-CT images of tibiae. Significance of results was determined using Student's *t* test.

Fig. 5. Qualitative and quantitative assessment of the effect of Apo2L/TRAIL treatment on normal bone. Representative three-dimensional reconstructed cross-sectional and longitudinal micro-CT images (5 μm resolution) of contralateral normal non-tumor-bearing tibiae from vehicle-treated and Apo2L/TRAIL-treated mice. The antiresorptive bisphosphonate zoledronic acid (ZOL) was used as a positive control for comparison in a separate cohort of animals ($n = 10$). Bone morphometric parameters including total bone volume and trabecular bone volume were assessed using micro-CT software as described in Materials and Methods. The extended evaluation of bone morphometric parameters is shown in Table 2. Data indicate that treatment with zoledronic acid (100 mg/kg/dose once weekly for 5 wk) resulted in significant changes in all bone morphometric parameters as expected. In contrast, treatment with Apo2L/TRAIL was without effect.



Despite this, the efficacy of Apo2L/TRAIL treatment on myeloma burden in bone and myeloma-induced bone destruction has not been reported. Our *in vitro* experiments confirmed that only two of seven myeloma cell lines (RPMI-8226 and KMS-11) were highly sensitive to the apoptotic effects of Apo2L/TRAIL. We then evaluated the antimyeloma effects of Apo2L/TRAIL in a murine model of myeloma-induced osteolysis in which RPMI-8226 or KMS-11 cells were injected into the intratibial space of immunodeficient mice. A limitation in measuring tumor burden in bone is that it is not possible to accurately assess the progression of tumor growth by palpation as in soft tissue tumors, because these tumors cannot be felt before they break through the cortical bone. To overcome this limitation, we used noninvasive BLI, which enabled extremely sensitive tracking of myeloma burden in bone in real-time before and after treatment in live animals. In addition, the micro-CT imaging not only allowed a precise qualitative description of Apo2L/TRAIL treatment effects on bone architecture but also provided quantitative bone morphometry. Using this methodology, we showed that Apo2L/TRAIL treatment reduced myeloma burden within the bone marrow and significantly protected the bone from myeloma-induced osteolysis in two sensitive myeloma cell lines. Histologic assessment of Apo2L/TRAIL-treated animals revealed the induction of apoptosis in a substantial fraction of the tumor within the marrow cavity, consistent with the decrease in bioluminescence. The bioavailability of Apo2L/TRAIL when administered via the peritoneal cavity, as in this study, is $\sim 30\%$ and the peak plasma levels expected with 30 mg/kg intraperitoneal dose given over 5 days is $\sim 7 \mu\text{g/mL}$.⁵ This is well within the range previously shown to have efficacy *in vivo* (22). However, prolonged treatment with Apo2L/TRAIL failed to completely eradicate tumors from the bone microenvironment, suggesting that higher doses and/or more frequent drug administration may be required to achieve complete eradica-

tion of tumors from the bone, because resistance appeared to develop with prolonged treatment. Development of resistance to Apo2L/TRAIL in the RPMI 8226 was not explained by differences in receptor expression between sensitive and resistant cells, indicating that other factors in the apoptotic pathways may be involved. These findings are consistent with our previously published studies, in which we have shown that Apo2L/TRAIL treatment reduced tumor burden and prevented breast cancer-induced bone destruction in an animal model of breast cancer growth in bone. However, prolonged treatment *in vivo* with Apo2L/TRAIL also resulted in the selection of breast cancer cells that were resistant to Apo2L/TRAIL, ultimately resulting in late recurrence (33). A limitation of the current study is that only two of seven the multiple myeloma cell lines tested were shown to be highly sensitive to Apo2L/TRAIL-induced apoptosis, suggesting that a combinatorial approach will be required to improve the therapeutic potential or to reverse resistance in future Apo2L/TRAIL-based therapies for multiple myeloma.

The current literature presents many inconsistencies regarding the activity of different versions of recombinant soluble Apo2L/TRAIL in modulating the differentiation and activity of bone resorbing osteoclasts. Recent studies showed the ability of these Apo2L/TRAIL versions to inhibit both human and mouse osteoclastogenesis as well as influence the survival of mature osteoclasts (36–38). In addition, recent work by Zauli et al. showed that injection of mice with recombinant Apo2L/TRAIL induced a significant increase in tibial trabecular thickness and total bone mass, leading this group to suggest that, in addition to its effects on cancer cells, Apo2L/TRAIL may regulate normal bone metabolism via inhibition of host osteoclast differentiation and bone resorption; however, an increase in trabecular thickness is more likely to be due to enhanced osteoblast activity (36). In contrast, other studies have suggested that different versions of recombinant Apo2L/TRAIL might promote osteoclastogenesis (8) and different molecular mechanisms to explain these observations have been proposed, with the interplay between Apo2L/TRAIL and the RANKL/RANK/OPG

⁵ A. Ashkenazi, personal communication.

system being central to these findings (8). In this study, our detailed histomorphometric and micro-CT analysis of the contralateral non-tumor-bearing bones of Apo2L/TRAIL-treated animals showed no significant effect of Apo2L/TRAIL on any bone morphometric parameter. In contrast, treatment with the antiresorptive bisphosphonate zoledronic acid, which was used for comparison as a positive control, resulted in a significant increase in bone mass as expected (39). Recently, we reported on the effect of Apo2L/TRAIL on osteoclast differentiation and bone resorption using three independent *in vitro* models of osteoclastogenesis (39). We showed that Apo2L/TRAIL did not block RANKL-mediated osteoclast differentiation or bone resorption from human peripheral blood mononuclear cells or from the murine monocytic cell line, RAW264.7. Furthermore, Apo2L/TRAIL had no effect on bone resorption by mature osteoclasts isolated from human giant cell tumors of bone. In addition, we found that Apo2L/TRAIL could not reverse the anti-osteoclastogenic effect of recombinant Fc-OPG or native OPG produced by cancer cells, a finding substantiated by Zauli et al. (36). These results argue against a direct effect of Apo2L/TRAIL on osteoclast differentiation and activity and are in direct contrast to earlier studies. It is now well accepted that various preparations of recombinant Apo2L/TRAIL may have different biological activities, perhaps explaining the findings in osteoclasts (36–38), in addition to the toxicity reported previously in human hepatocytes (40). The specificity and purity of the soluble Apo2L/TRAIL protein used in the present study has been verified *in vitro* (13), in animal models *in vivo* (22, 23), and in human clinical trials (27, 28).

Previous studies have raised the possibility that the activity of soluble Apo2L/TRAIL may be abrogated in the bone microenvironment, where expression of the antagonistic decoy receptor for Apo2L/TRAIL, OPG, is high and speculated that recombinant soluble Apo2L/TRAIL may have limited use as a therapeutic agent for the treatment of skeletal malignancies (8, 10, 11). Our previously published data on the tumor-suppressive activity of Apo2L/TRAIL against breast cancer cell

growth in bone (33) together with our findings here that recombinant soluble Apo2L/TRAIL reduces myeloma burden within the bone microenvironment and protects the bone from myeloma-induced bone destruction argue against an inhibitory role of OPG in Apo2L/TRAIL-induced apoptosis *in vivo*. In addition, we have shown that the protective effects of recombinant soluble Apo2L/TRAIL on myeloma burden in bone and myeloma-induced osteolysis are due to the direct actions of the ligand on myeloma cells themselves within the bone microenvironment, resulting in the abrogation of the “vicious cycle” of myeloma-induced bone destruction. In conclusion, our study highlights the need to clinically evaluate Apo2L/TRAIL alone and in combination with other antimyeloma agents to improve the outcome in patients with multiple myeloma.

As an alternative to soluble Apo2L/TRAIL, antibodies specific for both Apo2L/TRAIL proapoptotic receptors DR4 and DR5 have been developed and have now entered early clinical trials (41–46). These activate Apo2L/TRAIL receptor-mediated apoptotic pathways in a manner similar to the soluble ligand and may have enhanced therapeutic potential owing to their prolonged half life *in vivo*. This, together with their non-OPG binding properties, potentially makes monoclonal antibodies effective therapeutic agent for the treatment of cancer in bone and their efficacy against multiple myeloma should also be investigated.

Disclosure of Potential Conflicts of Interest

No potential conflicts of interest were disclosed.

Acknowledgments

We thank Dr. Beiqing Pan for laboratory support, the University of Adelaide microscopy resources staff for assistance, and the Institute of Medical and Veterinary Science animal facility staff for the animal care assistance.

References

- Croucher PJ, Apperley JF. Bone disease in multiple myeloma. *Br J Haematol* 1998;103:902–10.
- Kyle RA, Rajkumar SV. Multiple myeloma. *Blood* 2008;111:2962–72.
- Zannettino AC, Farrugia AN, Kortesisid A, et al. Elevated serum levels of stromal-derived factor-1 α are associated with increased osteoclast activity and osteolytic bone disease in multiple myeloma patients. *Cancer Res* 2005;65:1700–9.
- Farrugia AN, Atkins GJ, To LB, et al. Receptor activation of nuclear factor- κ B ligand expression by human myeloma cells mediates osteoclast formation *in vitro* and correlates with bone destruction *in vivo*. *Cancer Res* 2003;63:5438–45.
- Heider U, Hofbauer LC, Zavrski I, Kaiser M, Jakob C, Sezer O. Novel aspects of osteoclast activation and osteoblast inhibition in myeloma bone disease. *Biochem Biophys Res Commun* 2005;338:687–93.
- Bouralexis S, Findlay DM, Evdokiou A. Death to the bad guys: targeting cancer via Apo2L/TRAIL. *Apoptosis* 2005;10:35–51.
- Ashkenazi A. Targeting death and decoy receptors of the tumour-necrosis factor superfamily. *Nat Rev Cancer* 2002;2:420–30.
- Vitovski S, Phillips JS, Sayers J, Croucher PJ. Investigating the interaction between osteoprotegerin and receptor activator of NF- κ B or tumor necrosis factor-related apoptosis-inducing ligand: evidence for a pivotal role for osteoprotegerin in regulating two distinct pathways. *J Biol Chem* 2007;282:31601–9.
- Truneh A, Sharma S, Silverman C, et al. Temperature sensitive differential affinity of TRAIL for its receptors: DR5 is the highest affinity receptor. *J Biol Chem* 2000;275:23319–25.
- Shipman CM, Croucher PJ. Osteoprotegerin is a soluble decoy receptor for tumor necrosis factor-related apoptosis-inducing ligand/Apo2 ligand and can function as a paracrine survival factor for human myeloma cells. *Cancer Res* 2003;63:912–6.
- Emery JG, McDonnell P, Burke MB, et al. Osteoprotegerin is a receptor for the cytotoxic ligand TRAIL. *J Biol Chem* 1998;273:14363–7.
- Walczak H, Miller RE, Ariail K, et al. Tumoricidal activity of tumor necrosis factor-related apoptosis-inducing ligand *in vivo*. *Nat Med* 1999;5:157–63.
- Ashkenazi A, Pai RC, Fong S, et al. Safety and anti-tumor activity of recombinant soluble Apo2 ligand. *J Clin Invest* 1999;104:155–62.
- Atkins GJ, Bouralexis S, Evdokiou A, et al. Human osteoblasts are resistant to Apo2L/TRAIL-mediated apoptosis. *Bone* 2002;31:448–56.
- Butler LM, Liapis V, Bouralexis S, et al. The histone deacetylase inhibitor, suberoylanilide hydroxamic acid, overcomes resistance of human breast cancer cells to Apo2L/TRAIL. *Int J Cancer* 2006;119:944–54.
- Griffith TS, Chin WA, Jackson GC, Lynch DH, Kubin MZ. Intracellular regulation of TRAIL-induced apoptosis in human melanoma cells. *J Immunol* 1998;161:2833–40.
- Degli-Esposti MA, Smolak PJ, Walczak H, et al. Cloning and characterization of TRAIL-R3, a novel member of the emerging TRAIL receptor family. *J Exp Med* 1997;186:1165–70.
- Keane MM, Ettenberg SA, Nau MM, Russell EK, Lipkowitz S. Chemotherapy augments TRAIL-induced apoptosis in breast cell lines. *Cancer Res* 1999;59:734–41.
- Zhang XD, Franco AV, Nguyen T, Gray CP, Hersey P. Differential localization and regulation of death and decoy receptors for TNF-related apoptosis-inducing ligand (TRAIL) in human melanoma cells. *J Immunol* 2000;164:3961–70.
- Zhang XD, Nguyen T, Thomas WD, Sanders JE, Hersey P. Mechanisms of resistance of normal cells to TRAIL induced apoptosis vary between different cell types. *FEBS Lett* 2000;482:193–9.
- Suliman A, Lam A, Datta R, Srivastava RK. Intracellular mechanisms of TRAIL: apoptosis through mitochondrial-dependent and -independent pathways. *Oncogene* 2001;20:2122–33.
- Kelley SK, Harris LA, Xie D, et al. Preclinical studies to predict the disposition of Apo2L/tumor necrosis factor-related apoptosis inducing ligand in humans:

- characterization of *in vivo* efficacy, pharmacokinetics, and safety. *J Pharmacol Exp Ther* 2001;299:31–8.
23. Jin H, Yang R, Fong S, et al. Apo2L ligand/tumor necrosis factor-related apoptosis-inducing ligand cooperates with chemotherapy to inhibit orthotopic lung tumor growth and improve survival. *Cancer Res* 2004;64:4900–5.
 24. Roth W, Isenmann S, Naumann U, et al. Locoregional Apo2L/TRAIL eradicates intracranial human malignant glioma xenografts in athymic mice in the absence of neurotoxicity. *Biochem Biophys Res Commun* 1999;265:479–83.
 25. Chinnaiyan AM, Prasad U, Shankar S, et al. Combined effect of tumor necrosis factor-related apoptosis-inducing ligand and ionizing radiation in breast cancer therapy. *Proc Natl Acad Sci U S A* 2000;97:1754–9.
 26. Gliniak B, Le T. Tumor necrosis factor-related apoptosis-inducing ligand's antitumor activity *in vivo* is enhanced by the chemotherapeutic agent CPT-11. *Cancer Res* 1999;59:6153–8.
 27. Pan Y. Application of pharmacodynamic assays in a phase 1a trial of Apo2L/TRAIL in patients with advanced tumours [abstract 3535]. *J Clin Oncol (ASCO)* 2007;25:3535.
 28. Yee L. A phase 1B safety and pharmacokinetic (PK) study of recombinant human Apo2L/TRAIL in combination with rituximab in patients with low-grade non-Hodgkin lymphoma [abstr 8078]. *J Clin Oncol (ASCO)* 2007;25:8078.
 29. Mitsiades CS, Treon SP, Mitsiades N, et al. TRAIL/Apo2L ligand selectively induces apoptosis and overcomes drug resistance in multiple myeloma: therapeutic applications. *Blood* 2001;98:795–804.
 30. Ponomarev V, Doubrovin M, Serganova I, et al. A novel triple-modality reporter gene for whole-body fluorescent, bioluminescent, and nuclear noninvasive imaging. *Eur J Nucl Med Mol Imaging* 2004;31:740–51.
 31. Zannettino AC, Rayner JR, Ashman LK, Gonda TJ, Simmons PJ. A powerful new technique for isolating genes encoding cell surface antigens using retroviral expression cloning. *J Immunol* 1996;156:611–20.
 32. Berlin O, Samid D, Donthineni-Rao R, Akeson W, Amiel D, Woods VL. Development of a novel spontaneous metastasis model of human osteosarcoma transplanted orthotopically into bone of athymic mice. *Cancer Res* 1993;53:4890–5.
 33. Thai le M, Labrinidis A, Hay S, et al. Apo2L/tumor necrosis factor-related apoptosis-inducing ligand prevents breast cancer-induced bone destruction in a mouse model. *Cancer Res* 2006;66:5363–70.
 34. Sims NA, Brennan K, Spaliviero J, Handelsman DJ, Seibel MJ. Perinatal testosterone surge is required for normal adult bone size but not for normal bone remodeling. *Am J Physiol Endocrinol Metab* 2006;290:E456–62.
 35. Sims NA, Clement-Lacroix P, Da Ponte F, et al. Bone homeostasis in growth hormone receptor-null mice is restored by IGF-I but independent of Stat5. *J Clin Invest* 2000;106:1095–103.
 36. Zauli G, Rimondi E, Stea S, et al. TRAIL inhibits osteoclastic differentiation by counteracting RANKL-dependent p27Kip1 accumulation in pre-osteoclast precursors. *J Cell Physiol* 2008;214:117–25.
 37. Zauli G, Rimondi E, Nicolini V, Melloni E, Celeghini C, Secchiero P. TNF-related apoptosis-inducing ligand (TRAIL) blocks osteoclastic differentiation induced by RANKL plus M-CSF. *Blood* 2004;104:2044–50.
 38. Roux S, Lambert-Comeau P, Saint-Pierre C, Lepine M, Sawan B, Parent JL. Death receptors, Fas and TRAIL receptors, are involved in human osteoclast apoptosis. *Biochem Biophys Res Commun* 2005;333:42–50.
 39. Labrinidis A, Liapis V, Thai le M, et al. Does Apo2L/TRAIL play any physiologic role in osteoclastogenesis? *Blood* 2008;111:5411–2.
 40. Lawrence D, Shahroksh Z, Marsters S, et al. Differential hepatocyte toxicity of recombinant Apo2L/TRAIL versions. *Nat Med* 2001;7:383–5.
 41. Adams C, Totpal K, Lawrence D, et al. Structural and functional analysis of the interaction between the agonistic and monoclonal antibody Apomab and the proapoptotic receptor DR5. *Cell Death Differ* 2008;15:751–6.
 42. Pacey S, Plummer RE, Attard G, et al. Phase 1 and pharmacokinetic study of HGS-ETR2, a human monoclonal antibody to TRAIL-R2, in patients with advanced solid malignancies [abstract B114]. AACR-NCI-EORTC International Conference on Molecular Targets and Cancer Therapies; Philadelphia, PA; 2005.
 43. Camidge D, Herbst RS, Gordon M, et al. A phase 1 safety and pharmacokinetic study of Apomab, a human DR5 agonistic antibody, in patients with advanced cancer [abstract]. *Proc ASCO* 2007;25:3582.
 44. Hotte SJ, Hirte HW, Chen EX, et al. HGS-ETR1, a fully human monoclonal antibody to the tumor necrosis factor-related apoptosis-inducing ligand death receptor 1 (TRAIL-R1) in patients with advanced solid cancer: results of a phase 1 trial [abstract]. *Proc ASCO* 2005;23:3052.
 45. Sikic BI, Wakelee HA, von Mehren M, et al. A phase 1b study to assess the safety of lexatimumab, a human monoclonal antibody that activates TRAIL-R2, in combination with gemcitabine, pemetrexed, doxorubicin or FOLFIRI [abstract]. *Proc ASCO* 2007;25:14006.
 46. Tolcher AW, Mita M, Meropol NJ, et al. Phase 1 pharmacokinetic and biologic correlative study of mapatumumab, a fully human monoclonal antibody with agonistic activity to tumour necrosis factor-related apoptosis-inducing ligand receptor-1. *J Clin Oncol* 2007;25:1390–5.

Clinical Cancer Research

Apo2L/TRAIL Inhibits Tumor Growth and Bone Destruction in a Murine Model of Multiple Myeloma

Agatha Labrinidis, Peter Diamond, Sally Martin, et al.

Clin Cancer Res 2009;15:1998-2009.

Updated version Access the most recent version of this article at:
<http://clincancerres.aacrjournals.org/content/15/6/1998>

Cited articles This article cites 45 articles, 22 of which you can access for free at:
<http://clincancerres.aacrjournals.org/content/15/6/1998.full#ref-list-1>

Citing articles This article has been cited by 5 HighWire-hosted articles. Access the articles at:
<http://clincancerres.aacrjournals.org/content/15/6/1998.full#related-urls>

E-mail alerts [Sign up to receive free email-alerts](#) related to this article or journal.

Reprints and Subscriptions To order reprints of this article or to subscribe to the journal, contact the AACR Publications Department at pubs@aacr.org.

Permissions To request permission to re-use all or part of this article, use this link
<http://clincancerres.aacrjournals.org/content/15/6/1998>.
Click on "Request Permissions" which will take you to the Copyright Clearance Center's (CCC) Rightslink site.